

1                    **SI for “Outsize Influence of Central American**  
2                    **Orography on Global Climate”**

3                    **Jane W. Baldwin<sup>1</sup>, Alyssa R. Atwood<sup>2</sup>, Gabriel A. Vecchi<sup>3,4</sup>, and David S.**  
4                    **Battisti<sup>5</sup>**

5                    <sup>1</sup>Lamont-Doherty Earth Observatory, Columbia University

6                    <sup>2</sup>Department of Earth, Ocean, and Atmospheric Science, Florida State University

7                    <sup>3</sup>Department of Geosciences, Princeton University

8                    <sup>4</sup>High Meadows Environmental Institute, Princeton University

9                    <sup>5</sup>Department of Atmospheric Sciences, University of Washington

---

Corresponding author: Jane W. Baldwin, [jbaldwin@ldeo.columbia.edu](mailto:jbaldwin@ldeo.columbia.edu)

10 **References**

11 Meehl, G. A., Senior, C. A., Eyring, V., Flato, G., Lamarque, J.-F., Stouffer, R. J.,  
12 ... Schlund, M. (2020, June). Context for interpreting equilibrium climate  
13 sensitivity and transient climate response from the CMIP6 Earth system  
14 models. *Science Advances*, 6(26), eaba1981. Retrieved 2021-02-10, from  
15 <https://advances.sciencemag.org/content/6/26/eaba1981> (Publisher:  
16 American Association for the Advancement of Science Section: Review) doi:  
17 10.1126/sciadv.aba1981

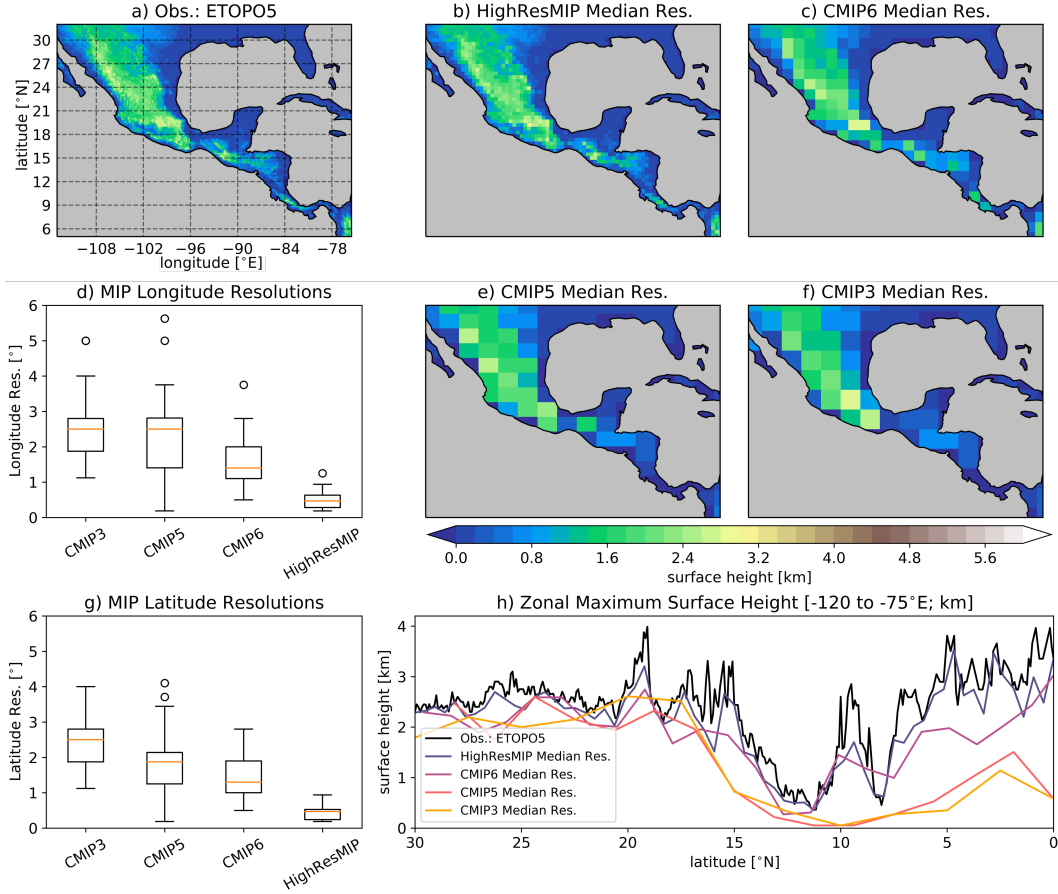


**Figure S1. Resolution of different model inter-comparison project (MIP) GCMs, and resolved topography at median MIP resolutions.** Maps of topography over Central America are plotted for observed ETOPO5 5' resolution topography (a), and ETOPO5 topography linearly regridded to the median atmosphere/land grid resolutions of HighResMIP (b), CMIP6 (c), CMIP5 (e), and CMIP3 (f). Zonal maximum surface height across Central America is plotted for ETOPO5 topography and the median resolution of the different MIPs (h). The range of approximate latitude and longitude resolutions of the different MIP GCMs are displayed as box and whisker plots (d,g), in which the red line represents the median, the top and bottom limits of the box are the lower quartile (Q1) and upper quartile (Q3), respectively, the whiskers represent the maximum and minimum values of the data that are not outliers, and the circles represent outliers defined as data points outside the range defined by  $[Q1 - 1.5 \times (Q3 - Q1)]$  and  $[Q3 + 1.5 \times (Q3 - Q1)]$ . While there is a significant range of resolutions across models in each MIP, model resolution has generally become finer over time, with median latitude by longitude resolutions being  $2.5^\circ \times 2.5^\circ$  for CMIP3,  $1.9^\circ \times 2.5^\circ$  for CMIP5,  $1.3^\circ \times 1.4^\circ$  for CMIP6, and  $0.47^\circ \times 0.47^\circ$  for HighResMIP. Resolutions for different MIP models were collected to the best of the authors' abilities by combining information from [https://pcmdi.llnl.gov/ipcc/model\\_documentation/ipcc\\_model\\_documentation.php](https://pcmdi.llnl.gov/ipcc/model_documentation/ipcc_model_documentation.php) for CMIP3 (25 GCMs), from <https://portal.enes.org/data/enes-model-data/cmp5/resolution> for CMIP5 (56 GCMs), from Meehl et al. (2020) and the Earth System Grid Federation (ESGF) archives <https://pcmdi.llnl.gov/CMIP6> for CMIP6 (41 GCMs), and from ESGF archives [https://pcmdi.llnl.gov/CMIP6/ArchiveStatistics/esgf\\_data\\_holdings/HighResMIP](https://pcmdi.llnl.gov/CMIP6/ArchiveStatistics/esgf_data_holdings/HighResMIP) for HighResMIP (19 GCMs). We removed from our analysis of HighResMIP lower resolution GCMs included for comparison to higher resolution GCMs, or those that overlap with CMIP6. Note that these resolutions are in many cases approximate— numerous included GCMs are spectral models or have grids that become finer in the tropics.

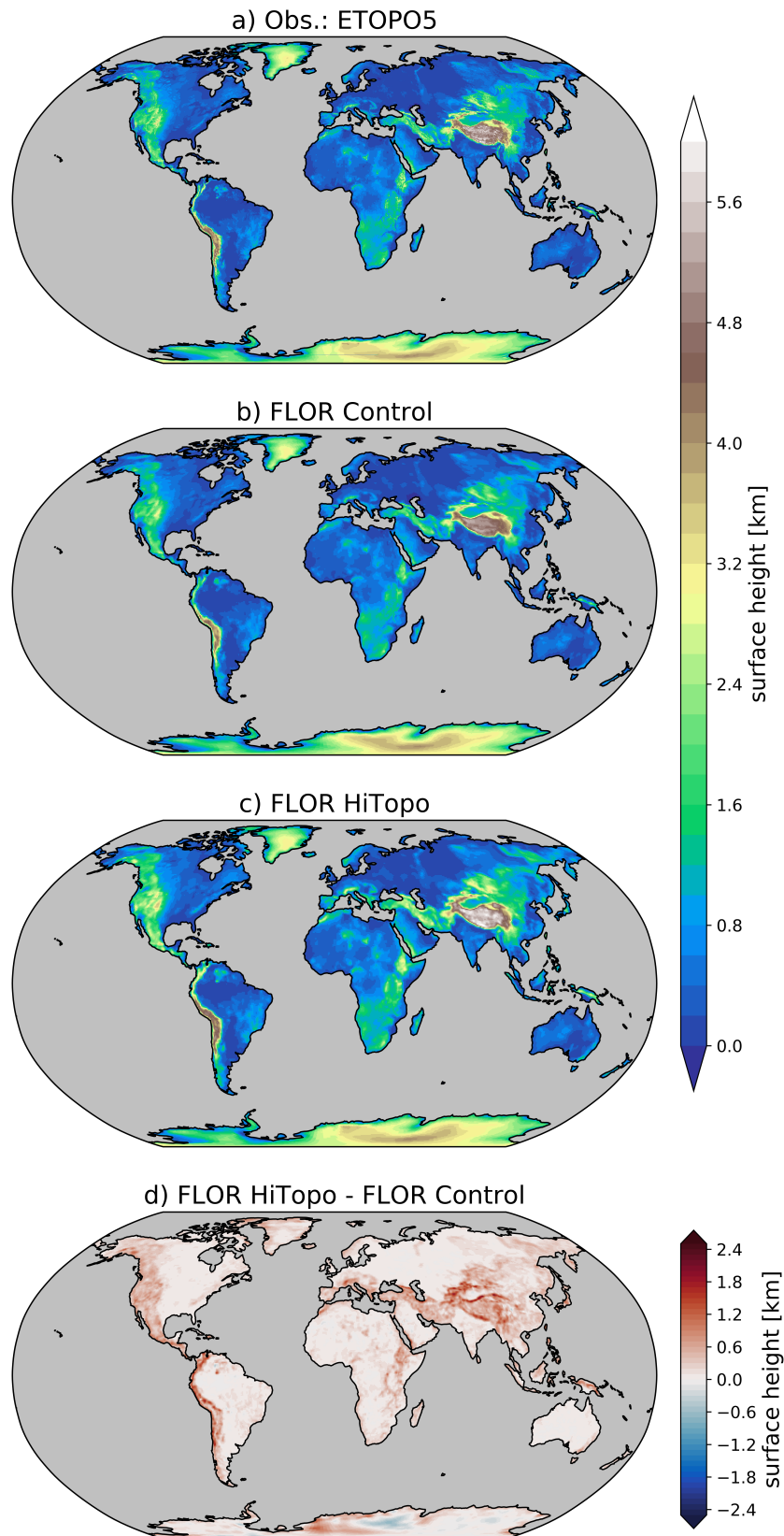


**Figure S2.** Surface height boundary conditions in observations compared to the **FLOR** simulations. From top to bottom, shown are the ETOPO5 5' resolution topography data (a), FLOR Control (b), FLOR HiTopo (c), and the difference between FLOR HiTopo and FLOR Control (d).

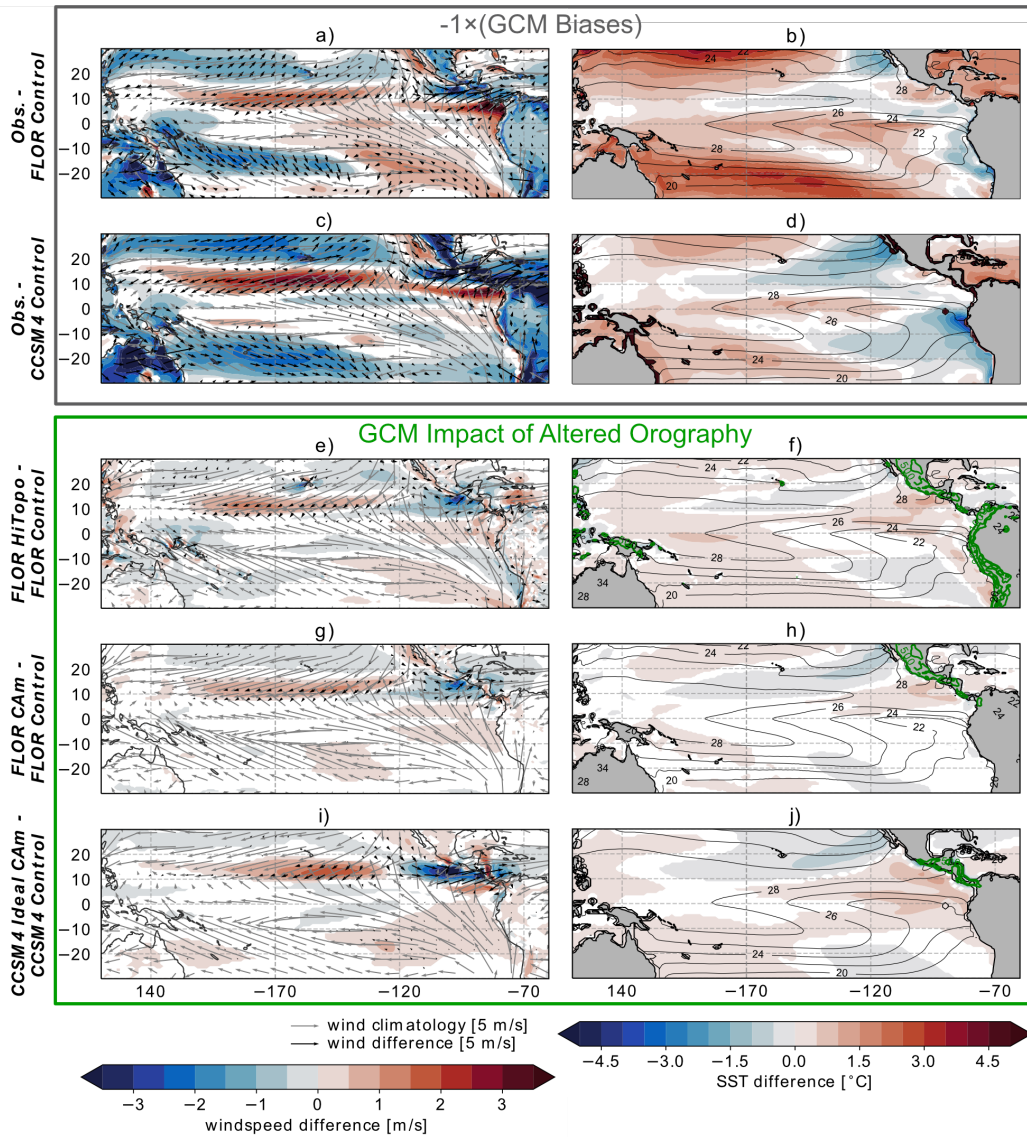


**Figure S3.** As in Fig. 3 but for September-November (SON): influence of orography on tropical Pacific winds and SSTs for SON. SON average wind vectors and speeds are shown in the left column (a,c,e,g,i), with windspeed differences shaded, wind differences in black vectors, and the relevant Control wind climatology in grey vectors. Wind data is taken from the lowest atmospheric level available in the 3-D data from the MERRA-2 reanalysis (“Obs.”– 1000 hPa), FLOR output (996.1 hPa), or CCSM4 output (992.6 hPa). SON average SSTs are shown in the right column (b,d,f,h,j) with SST differences shaded, and Control/Obs. climatology in black contours. The observed SST data is HadISST. In the lower right-column panels (f,h,j) the difference in the surface height boundary conditions between the relevant perturbation simulations and Control simulations is contoured in green. In all panels, differences that are not significant at a 90% level based on a two-sided  $t$ -test are masked out (i.e. are white for the filled contours, and do not appear for the vectors).

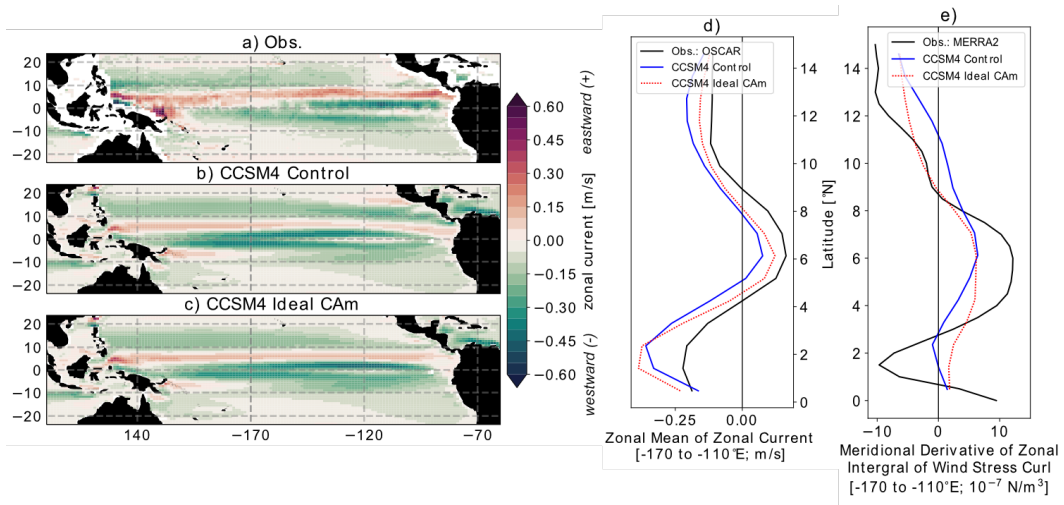


**Figure S4.** As in Fig. 4 but for CCSM4: zonal currents and related winds in CCSM4. Time mean zonal currents across the tropical Pacific are shaded for observations (OSCAR; a), CCSM4 Control (b), and CCSM4 Ideal CAM (c). Before plotting, the OSCAR data ( $0.33^\circ \times 0.33^\circ$ ) is regridded to the FLOR ocean grid. To highlight and understand changes in the north equatorial counter current (NECC), zonal means of these zonal currents are plotted for the northern tropics (d), and compared to the meridional derivatives of the zonal integrals of wind stress curl (e); in (d) and (e) observations are plotted in black, CCSM4 Control is blue, and CCSM4 Ideal CAM is dashed red.

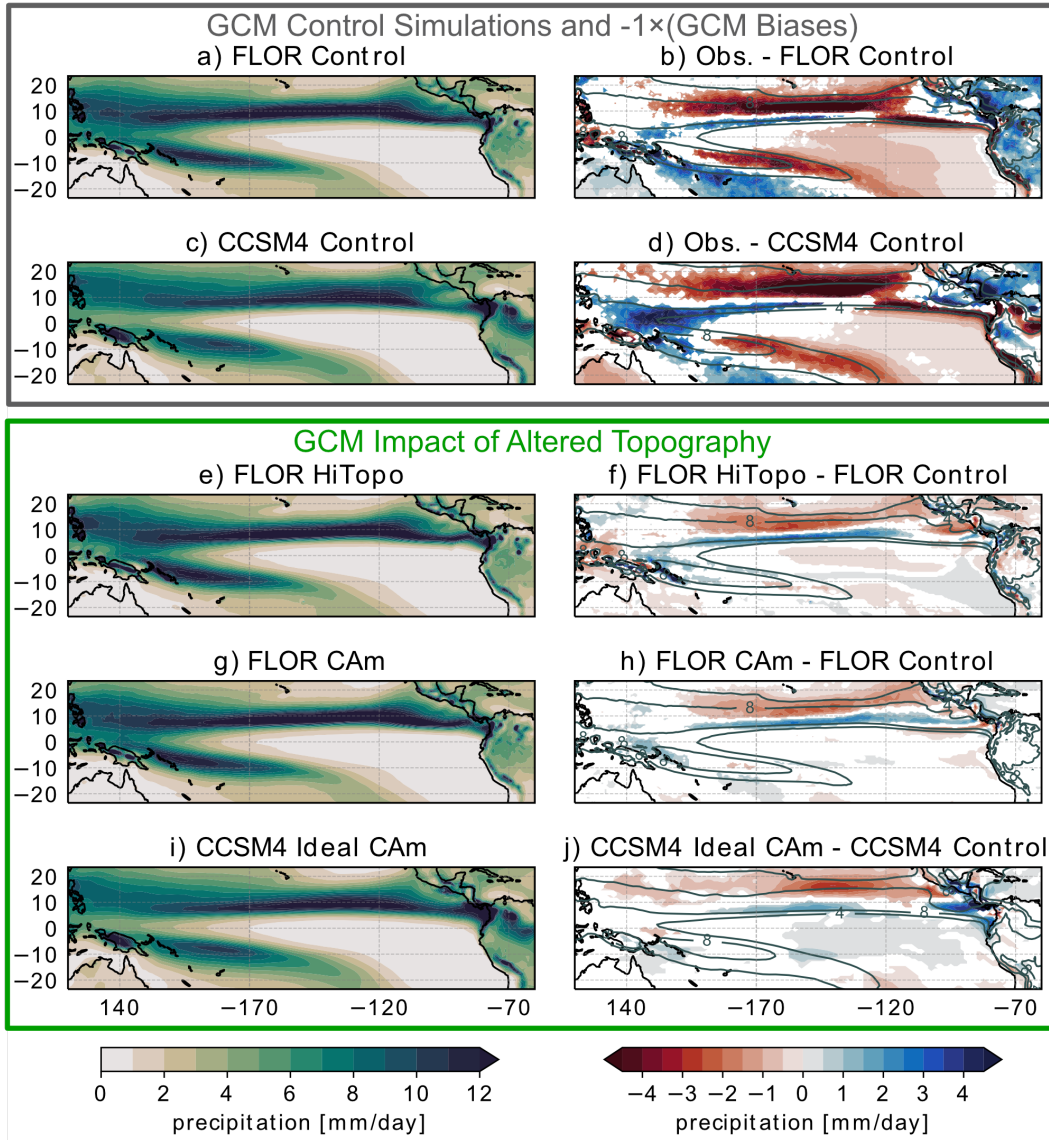


**Figure S5.** As in Fig. 5 but for SON: influence of high topography on precipitation in the tropical Pacific for SON. The left column shows SON seasonal mean precipitation over the tropical Pacific for each of the model runs– FLOR Control (a), CCSM4 Control (c), FLOR HiTopo (e), FLOR CAM (g), and CCSM4 Ideal CAM (i). The right column shows differences between SON seasonal mean precipitation for observations vs. Control simulations– Obs. vs. FLOR Control (b), Obs. vs. CCSM4 Control (d)– and altered topography vs. Control simulations– FLOR HiTopo vs. FLOR Control (f), FLOR CAM vs. FLOR Control (h), CCSM4 Ideal CAM vs. CCSM4 Control (j). In these right column difference panels (b,d,f,h,j), the corresponding FLOR or CCSM4 Control simulation SON precipitation climatology is contoured in dark gray-green, with contour labels in mm/day. In the right panels, differences that are not significant at a 90% level based on a two-sided  $t$ -test are masked white.

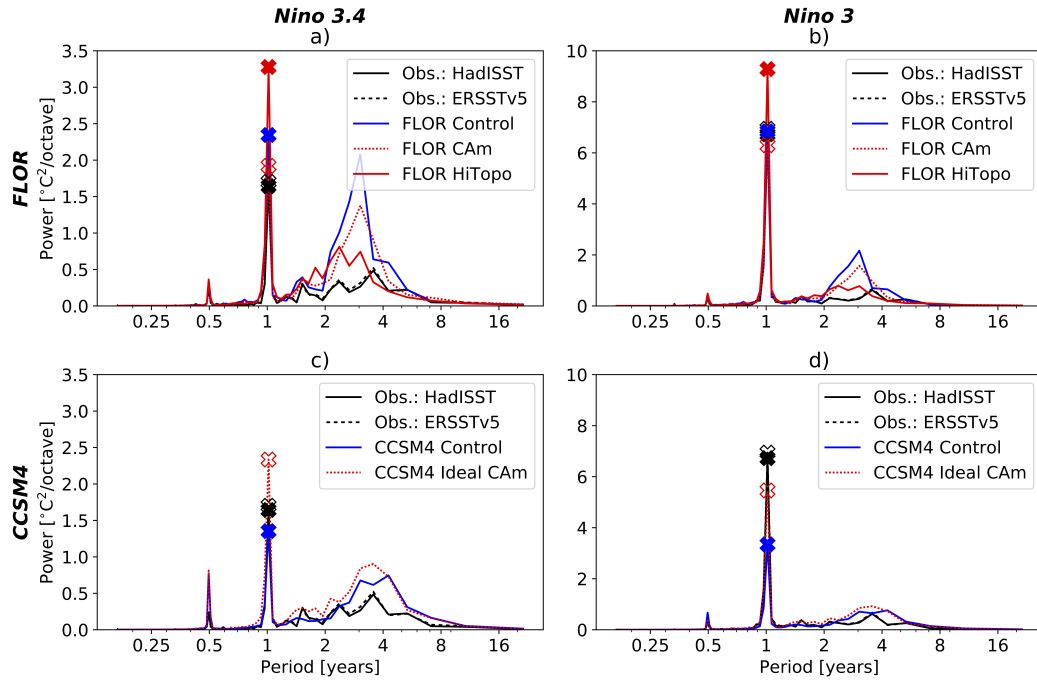


**Figure S6. ENSO power spectra for GCM simulations and observations.** Power spectra of the Niño 3.4 (left column), and Niño 3 (right column) SST anomalies. In all panels HadISST observations are shown in black; in the top panels, FLOR Control is blue, FLOR CAm is dashed red, and FLOR HiTopo is solid red; in the bottom panels, CCSM4 Control is blue and CCSM4 Ideal CAm is dashed red. The power at annual frequencies is highlighted with  $\times$ -symbols, with colors corresponding to the lines.

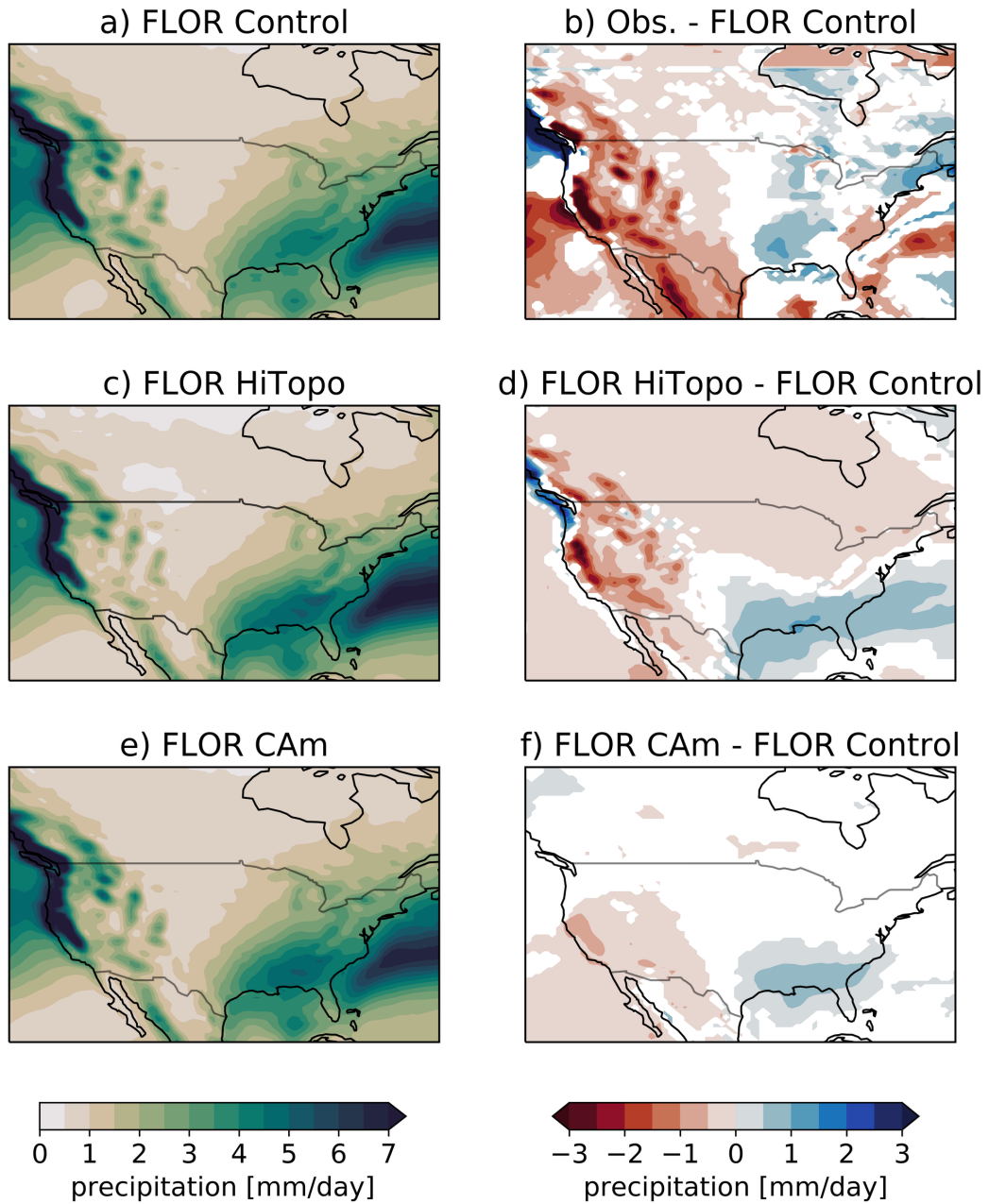


**Figure S7. Influence of high orography on precipitation across North America for December-February (DJF).** The left column shows DJF seasonal mean precipitation over North America for each of the FLOR model runs– FLOR Control (a), FLOR HiTopo (c), and FLOR CAM (e). The right column shows the difference in DJF seasonal mean precipitation for observations vs. FLOR Control (b), FLOR HiTopo vs. FLOR Control (d), and FLOR CAM vs. FLOR Control. In the right panels, differences that are not significant at a 90% level based on a two-sided *t*-test are masked white.